catalysts

MDPI

Article

Thermal Conversion of Sugarcane Bagasse Coupled with Vapor Phase Hydrotreatment over Nickel-Based Catalysts: A Comprehensive Characterization of Upgraded Products

Tarcísio Martins Santos [1], Wenes Ramos da Silva [1], Jhonattas de Carvalho Carregosa [1], Caroline Carriel Schmitt [2], Renata Moreira [3], Klaus Raffelt [2,*], Nicolaus Dahmen [2] and Alberto Wisniewski, Jr. [1,*]

[1] Petroleum and Energy from Biomass Research Group (PEB), Department of Chemistry, Federal University of Sergipe, São Cristóvão 49100-000, Sergipe, Brazil; tarcisiom249@outlook.com (T.M.S.); wenes.rms1@gmail.com (W.R.d.S.); jhonattas.carregosa@live.com (J.d.C.C.)
[2] Institute of Catalysis Research and Technology, Karlsruhe Institute of Technology, 76344 Karlsruhe, Germany; caroline.schmitt@partner.kit.edu (C.C.S.); nicolaus.dahmen@kit.edu (N.D.)
[3] Laboratory of Bioenergy and Energy Efficiency, Institute for Technological Research, IPT, São Paulo 05508-901, São Paulo, Brazil; renatam@ipt.br
* Correspondence: klaus.raffelt@kit.edu (K.R.); albertowj@academico.ufs.br (A.W.J.)

Abstract: In the present work, we compared the chemical profile of the organic compounds produced in non-catalytic pyrolysis of sugarcane bagasse at 500 °C with those obtained by the in-line catalytic upgrading of the vapor phase at 350 °C. The influence over the chemical profile was evaluated by testing two Ni-based catalysts employing an inert atmosphere (N_2) and a reactive atmosphere (H_2) under atmospheric pressure with yields of the liquid phase varying from 55 to 62%. Major changes in the chemical profile were evidenced in the process under the H_2 atmosphere, wherein a higher degree of deoxygenation was identified due to the effect of synergistic action between the catalyst and H_2. The organic fraction of the liquid phase, called bio-oil, showed an increase in the relative content of alcohols and phenolic compounds in the GC/MS fingerprint after the upgrading process, corroborating with the action of the catalytic process upon the compounds derived from sugar and carboxylic acids. Thus, the thermal conversion of sugarcane bagasse, in a process under an H_2 atmosphere and the presence of Ni-based catalysts, promoted higher deoxygenation performance of the pyrolytic vapors, acting mainly through sugar dehydration reactions. Therefore, the adoption of this process can potentialize the use of this waste biomass to produce a bio-oil with higher content of phenolic species, which have a wide range of applications in the energy and industrial sectors.

Keywords: hydropyrolysis; hydrodeoxygenation; catalytic reform; sugarcane industries; fast pyrolysis; bio-oilomics; mass spectrometry

Citation: Santos, T.M.; Silva, W.R.d.; Carregosa, J.d.C.; Schmitt, C.C.; Moreira, R.; Raffelt, K.; Dahmen, N.; Wisniewski, A., Jr. Thermal Conversion of Sugarcane Bagasse Coupled with Vapor Phase Hydrotreatment over Nickel-Based Catalysts: A Comprehensive Characterization of Upgraded Products. *Catalysts* **2022**, *12*, 355. https://doi.org/10.3390/catal12040355

Academic Editor: Claudia Carlucci

Received: 14 February 2022
Accepted: 18 March 2022
Published: 22 March 2022

1. Introduction

The challenges concerning the energy and industrial security of the future, and the environmental problems related to the use of fossil fuels, have directed the pursuit of energy and industrial chemical supplies to a matrix that is environmentally friendly and widely available, such as biomass [1]. Due to its high abundance and potential for the production of fuels and biochemicals, biomass became the foundation of today's renewable energy [2]. The sugar and ethanol industries play a significant role in the global economy and the production of an important lignocellulosic residue, the sugarcane bagasse (SCB) [3]. SCB is one of the main agricultural residues produced in Brazil, which is the world leader in sugarcane production with approximately 592 million tons produced in 2021 [4]. If we consider that during the sugarcane processing, approximately 27% of bagasse is generated, the production of SCB in Brazil in the year 2021 was equivalent to 160 million tons [5].

As a fibrous residue, with high volatile organic material content and low percentages of ash and sulfur, SCB, through its thermal conversion, is an important biomass source for

the renewable energy sector as well as for the chemical industry [6]. According to Schmitt et al. [7], the use of SCB as a biomass source is particularly advantageous compared to other wastes, since it is already produced and collected within the sugar refinery, which would facilitate the implementation and integration of a process to convert biomass into bio-oil in the sugarcane processing industry itself. Therefore, research into new technologies for the conversion of sugarcane bagasse, or the study of the influence of modifications to existing technologies, should be emphasized.

Pyrolysis is one of the most promising thermal conversion processes for producing value-added products from biomass [8]. The pyrolysis process consists of the thermal degradation of organic matter, in an inert atmosphere, to form pyrolytic gas, biochar, and a liquid product, described as bio-oil, which is composed of an aqueous and an organic phase [9]. Bio-oil is the main product obtained from the rapid pyrolysis of biomass and has been considered as a potential renewable substitute to minimize the current dependence on petroleum derivatives [10]. However, due to the low selectivity in the pyrolysis process, the bio-oil produced presents an extremely complex composition and characteristics that significantly hinder its direct use as fuel or chemicals, among them we can highlight the high water content and high oxygen content, which gives the product a high chemical and thermal instability, acid properties, and tendency to polymerization [11,12]. In this context, aiming at the production of improved bio-oils, either less oxygenated or enriched in compounds of interest for the industry, such as phenolic compounds, which, if produced from a renewable material, can serve as an alternative to those derived from the oil industry, some modifications to the pyrolysis process have been proposed in recent years [13,14].

Among them, the use of catalysts has proven to be a promising route. The process of catalytic pyrolysis can occur in two different ways, in the in situ mode, in which the catalyst is in direct contact with the biomass, the process is isothermal, and the catalyst acts over biomass and vapor phase at the same time, and in the ex situ configuration, in which the catalyst does not come in contact with the biomass, acting only over the vapor phase from biomass pyrolysis occurring often at different temperatures [15]. Thus, the catalytic pyrolysis process aims to improve the quality of the obtained bio-oil [13]. In this procedure, the improvement of the quality of the bio-oil, through its deoxygenation, occurs mainly via decarboxylation mechanisms, in which the oxygen from the molecules is removed in the form of carbon dioxide (CO_2); decarbonylation, in which the oxygen is released in the form of carbon monoxide (CO); and by dehydration, in which the formation of water (H_2O) acts as a marker of this reaction pathway [16]. Nevertheless, the catalytic pyrolysis process has major limitations, which are related to the accumulation of coke on the surface of the catalysts, as well as a low carbon efficiency, since a large amount of carbon in the pyrolytic vapors is converted into coke and gases such as CO_2 and CO, resulting in a lower yield of bio-oil, which usually still contains significant levels of oxygen [14]. Therefore, to solve the problems mentioned above, the modification of the inert atmosphere of the pyrolytic systems into a reactive hydrogen atmosphere favors the cracking of biomass, and in conjunction with the use of catalysts in a process called catalytic hydropyrolysis, through deoxygenation and hydrogenation reactions, promotes the production of a bio-oil of better quality [10,17].

The addition of catalysts to the hydropyrolysis process is essential to increase the carbon efficiency and reduce coke accumulation on the catalyst surface, because the synergistic effect between catalyst and hydrogen atmosphere minimizes the occurrence of polymerization/condensation reactions, and consequently reduces the formation of coke precursors [18]. The catalytic agent plays an important role in the hydrodeoxygenation and catalytic reforming reactions of bio-oil, and for this reason, the selection and development of catalysts for the hydrothermal treatment of bio-oils have been the subject of several investigations [19]. Several noble metal catalysts, such as Ru, Pt, Mo, Pd, and Co, show promise in catalytic processes. However, low availability and high cost are limiting factors from an industrial point of view. Differently, nickel (Ni)-based catalysts have been shown to be active in the catalytic treatment of bio-oils, and have been considered the most promising

due to their high activity and affordability [7,20]. By applying Ni catalysts supported on zeolites in the catalytic hydropyrolysis process of waste coffee powder, Ren et al. [21] reported that by promoting macromolecule hydrocracking, alkylation, cyclization, and aromatization reactions, the catalysts assisted in the production of a less oxygenated bio-oil with higher aromatic hydrocarbon content. This result corroborates the work of Zhou et al. [22], where the authors, when investigating the activity of Ni-based catalysts in the process of deoxygenation of vapors produced from the hydropyrolysis of *Camellia sinensis* residues, reported the production of a bio-oil 88% less oxygenated, and with high content of chemical compounds of the energy matrix.

Nevertheless, although these are widespread catalysts, their use in the catalytic hydrolysis process of sugarcane bagasse is still poorly explored. In this context, this work investigated the influence of the reaction atmosphere over the chemical profile of organic compounds in the non-catalytic thermochemical conversion process as well as the catalytic upgrading of the vapor phase by evaluating two Ni-based catalysts also over an inert (N_2) and reactive (H_2) atmosphere. The molecular behavior of the chemicals produced during the different processes was discussed, and the results of this research should be of assistance in the proposition, implementation, and integration of bagasse conversion processes in sugarcane industries to produce renewable-based chemicals, such as phenolic compounds. To date, this is the first work to perform a comprehensive molecular characterization to evaluate the catalytic hydropyrolysis process of sugarcane bagasse using nickel-based catalysts.

2. Results and Discussion

2.1. Influence of the Processes on Product Distribution and Elemental Composition of Biochar

The non-catalytic and catalytic pyrolysis and hydropyrolysis experiments of SCB were performed using a microreactor arranged horizontally, consisting of two in-line furnaces, where the first was responsible for cracking the biomass at 500 °C and the second for the ex-situ catalytic upgrading of the pyrolytic vapors at 350 °C. Both processes were carried out under atmospheric pressure. Two Ni-based catalysts, one commercially available and another prepared by the wet impregnation method, were used for the pyrolytic vapors upgrading reactions. The commercially available catalyst, described as Ni-Cr (specific surface area of 94 $m^2\ g^{-1}$), is composed of 30 wt % Ni, 26 wt % NiO, 15 wt % Cr_2O_3, and 1.5 wt % graphite, supported on diatomaceous earth. The second catalyst, Ni/SiO_2 (specific surface area of 215 $m^2\ g^{-1}$), is composed of 7.9 wt % Ni, supported on SiO_2. The average particle size of each catalyst was estimated by the Scherrer equation, through X-ray diffraction analysis. The Ni/SiO_2 catalyst had a value of 17.7 nm, while the Ni-Cr catalyst had a value of 4.4 nm. More details on the catalysts used are available in the previous work of Schmitt et al. [7].

Because this is a reactor composed of two connected furnaces operating at different temperatures, the connection point between furnace 1 and furnace 2 was described as the interface zone. Since the reactor was laid out horizontally, a fraction of the vapors produced from the thermal conversion of biomass, in oven 1, condensed and remained static in this interface zone, and this fraction was not affected by the catalytic reforming process, which occurred in oven 2, since it did not interact with the catalyst bed. This fraction was defined as the Heavy Liquid Fraction (HLF) as it consists of condensable organic compounds at a temperature of 350 °C. The light liquid fraction (LLF) is the fraction that condenses after the second furnace, at the exit of the reactor.

To determine the statistical significance between yields of the products obtained by the different processes, the statistical treatment of the analysis of variance (ANOVA) was used, considering a 95% confidence level, followed by the Tukey post hoc test [23,24]. Table 1 shows the yields of the non-catalytic and catalytic thermal conversion products of SCB under N_2 and H_2 atmosphere, and Figure S2 of the Supplementary Materials describes the results of the statistical test performed for each product separately.

Table 1. Non-catalytic and catalytic pyrolysis and hydropyrolysis product yields.

Sample	LLF (wt %)	Gases (wt %)	HLF (wt %)	Biochar (wt %)
(N_2)—SCB	61.83 ± 1.57	16.15 ± 1.29	1.68 ± 0.36	20.34 ± 0.92
(H_2)—SCB	60.06 ± 0.96	17.22 ± 0.52	1.43 ± 0.06	21.29 ± 1.00
(N_2)—SCB+Ni/SiO_2	56.25 ± 0.69	20.88 ± 1.04	1.82 ± 0.32	21.04 ± 0.61
(H_2)—SCB+Ni/SiO_2	56.53 ± 0.35	19.58 ± 0.39	1.57 ± 0.16	22.32 ± 0.66
(N_2)—SCB+Ni-Cr	55.13 ± 1.51	21.78 ± 0.65	1.96 ± 0.20	21.13 ± 1.00
(H_2)—SCB+Ni-Cr	54.93 ± 0.41	22.39 ± 0.82	1.49 ± 0.13	21.19 ± 1.34

The pyrolysis of sugarcane bagasse in the inert atmosphere has been evaluated in several studies in the literature; the yields obtained here—55–65 wt % liquids, 15–25 wt % gases, and approximately 20 wt % solids—are in agreement with those reported in the review by Toscano Miranda et al. [5]. Considering the change to the H_2 atmosphere and use of catalysts during the vapor phase upgrading, it was observed that only the LLFs and gases produced during the upgrading processes were significantly affected for both atmospheres, N_2 and H_2. ANOVA revealed that switching the reaction atmosphere from N_2 to H_2 in the non-catalytic process, i.e., comparing (N_2)—SCB with (H_2)—SCB, was not able to significantly alter the distribution of the products obtained. According to Resende [25], the replacement of the inert atmosphere of a fast pyrolysis system by a reactive hydrogen atmosphere at atmospheric pressure, as used in this study, is not able to exert a strong influence on the products obtained, which highlights the importance of adding a catalyst to promote improvement in bio-oil quality. However, at high pressures, as described by Jan et al. [26], the influence of the H_2 atmosphere on product yields is higher when compared to those obtained under an inert atmosphere, promoting greater gas formation during the process.

Evaluating the influence of the catalysts on the experiments over an inert atmosphere and adopting the non-catalytic pyrolysis experiment as a control, it was observed that the addition of the catalysts to the reaction system resulted in a significant decrease in the yield of LLFs and an increase in the gases (Figure S2). Regarding the LLF obtained in the non-catalytic pyrolysis, it was observed that the SCB conversion was 61.83 wt %. When the Ni/SiO_2 catalyst was used, starting with an LLF yield of 56.25 wt %, a ≈9% reduction in the yield of this product was determined compared to the control experiment, while the addition of the Ni-Cr catalyst (55.13 wt % in LLF) caused a ≈11% reduction in the conversion of biomass into LLF. Concerning the gases produced, a linear trend was observed that was inversely proportional to the decrease in LLFs obtained in the catalytic pyrolysis. The use of Ni/SiO_2 and Ni-Cr catalysts promoted a gas yield of 20.88 wt % and 21.78 wt %, respectively, and when comparing these values with the yield of this product in the non-catalytic pyrolysis process (16.15 wt % in gases), they represent increases of ≈29 and ≈34%, respectively. Considering that only the LLFs and gases from the processes passed through the catalyst bed, we suggest that the catalysts have promoted an enhanced cracking of the compounds contained in the light liquid fraction, which has resulted in the increased formation of gaseous compounds when compared to the yield of the non-catalytic process [27,28]. When comparing the LLFs and gases produced in the catalytic processes, no statistically significant differences were observed between the yields of the products obtained in (N_2)—SCB+Ni/SiO2 and (N_2)—SCB+Ni-Cr.

With respect to the process under the H_2 atmosphere, the addition of the catalysts to the process had a significant influence on the yields of LLFs and gases, as shown in Figure S2 of the Supplementary Materials. In the non-catalytic hydropyrolysis, there was determined the conversion of biomass to LLF equivalent to 60.06 wt %. Whereas a decrease of ≈6% was observed for the yield of the referred product when the Ni/SiO_2 catalyst was employed (56.53 wt % in LLF). Regarding the Ni-Cr catalyst (54.93 wt % in LLF), a reduction in the yield of LLF of ≈9% was determined. Similarly, to what was determined in the inert atmosphere experiments, when using catalysts in the reactive atmosphere processes, the same trend of reduced LLF yield and subsequent increase in the gas fraction was noticed. In

the non-catalytic hydropyrolysis experiment, the gas production amounted for 17.22 wt %. In the catalytic processes, yields of 19.58 wt % and 22.59 wt % were determined when using Ni/SiO_2 and Ni-Cr catalysts, respectively. In comparison with the activity of the Ni/SiO_2 catalyst, a higher production of gaseous compounds was observed in the Ni-Cr catalyzed process, suggesting a higher activity in the hydropyrolysis process. The higher nickel content present in this catalyst (≈6 times higher) was attributed as the determining factor for the observed changes since the nickel content present in catalysts exhibits a strong influence on their activity [29]. Furthermore, a higher nickel content promotes a higher acidity of the catalyst, which helps increase the degree of deoxygenation and secondary cracking of the vapors, thus reducing the yield of the liquid fraction and, consequently, increasing the gas fraction [30,31].

With respect to the yields of the HLFs and biochars produced, these products were not affected by the action of the catalysts, as they do not interact with the catalyst bed, and considering that the only changes of the reactor atmosphere from N_2 to H_2, under atmospheric pressure, did not influence such products, the yields of HLFs and biochars remained unchanged. This observation corroborates the results obtained from the elemental analysis of biochar samples, presented in Table 2.

Table 2. Elemental biochar analysis.

Sample	C (wt %)	H (wt %)	N (wt %)	O (wt %) [a]	Ash (wt %)
(N_2)—SCB	69.48	3.08	0.92	15.74	10.78
(H_2)—SCB	69.28	2.98	0.85	17.07	10.00
(N_2)—SCB+Ni/SiO_2	69.55	2.77	0.84	16.64	9.97
(H_2)—SCB+Ni/SiO_2	68.91	2.82	0.84	18.01	9.90
(N_2)—SCB+Ni-Cr	69.93	2.64	0.99	16.37	9.43
(H_2)—SCB+Ni-Cr	69.33	3.08	0.85	16.78	9.96

[a] Determined by the difference.

The biochars produced during the processing of SCB, in an inert and reactive atmosphere, presented similar compositions, evidencing that the evaluated processes did not influence the composition of this product. Both samples presented average elemental percentages of 69.4 wt % of C, 2.9 wt % of H, 0.88 wt % of N, and 16.8 wt % of O. From the implementation of a thermal conversion process of SCB in sugarcane industries, the produced biochar can be destined to soil applications, thus improving the production capacity of sugarcane, as well as in applications for energy generation for industry [32,33]. On the basis of the observation that the gases and LLFs were the only ones influenced by the processes, to evaluate the effect of the atmosphere alteration and catalyst insertion over the chemical composition of these products, we conducted analyses for chemical characterization. The gases were analyzed by GC-TCD, and the LLFs produced by the different processes were characterized by GC/MS, for characterization of volatilizable species, and by HESI(±)-FT-Orbitrap MS for analysis of semi-volatile and non-volatilizable polar components.

2.2. Effect of the Processes upon the Composition of the Gaseous Products

Through the analysis of the non-condensable products, the following gases were detected in their composition: CO_2, CO, H_2, and CH_4. The results obtained in the quantification of these species in the samples are presented in Figure 1, which are expressed in terms of the amount of matter per kilogram of pyrolyzed SCB (mol kg_{SCB}^{-1}). Details about the statistical significance of the results of the analyses are available in Figure S2 of the Supplementary Materials. When evaluating the influence that the atmosphere had upon the chemical composition of the gaseous products, no significant changes were found in the quantity of gases formed in the pyrolysis at the N_2 atmosphere and hydropyrolysis (H_2) process, suggesting that the gas samples produced by these two processes are chemically equal. It is worth noting that the H_2 gas was not monitored in the hydropyrolysis process, since it was the species responsible for the reaction atmosphere.

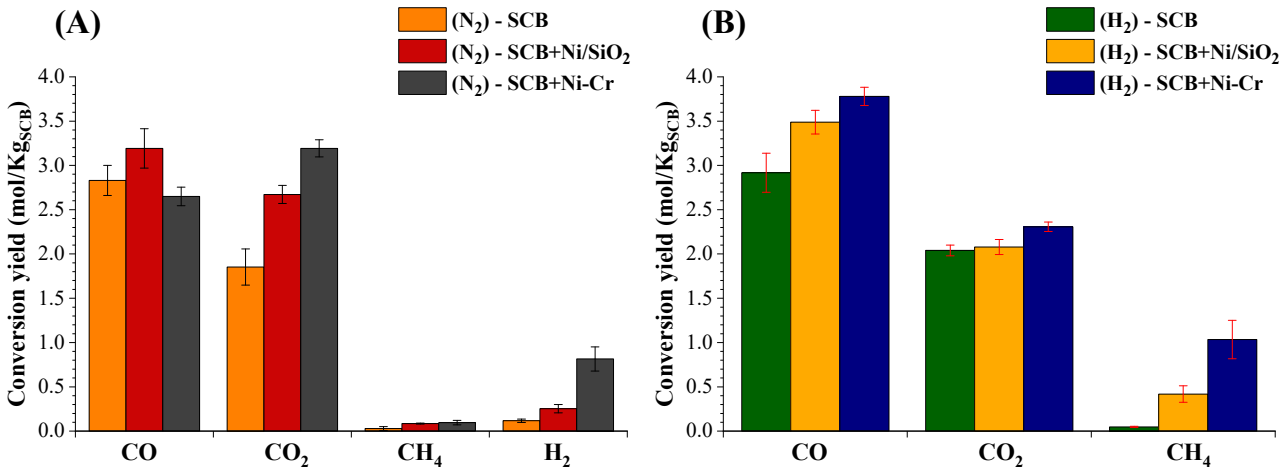

Figure 1. Composition of the gaseous products: (**A**) non-catalytic and catalytic pyrolysis and (**B**) non-catalytic and catalytic hydropyrolysis.

Assessing the influence of catalysts on the process in the N_2 atmosphere (Figure 1A) and adopting the non-catalytic pyrolysis experiment as a control, the usage of the catalysts was observed to promote a higher formation of CO_2 and H_2, while the production of CO and CH_4 gases was not significantly affected (Figure S2). The production of CO_2 in the non-catalyzed pyrolysis was ≈2 mol $kg_{SCB}{}^{-1}$ and of H_2 was 0.12 mol $kg_{SCB}{}^{-1}$. In the Ni/SiO_2-catalyzed process, a ≈44% increase in CO_2 yield was observed, and a ≈116% increment in H_2 was produced. When the Ni-Cr catalyst was used, the amount of CO_2 produced was increased by ≈72%, and that of H_2 was raised by ≈634%. This result suggests that in the catalytic pyrolysis process, nickel acted mainly through decarboxylation routes, promoting CO_2 formation through the cracking of RCO_2H functional group molecules, such as carboxylic acids and multifunctional structures present in the bio-oil, and via aromatization, explained by the increased production of H_2 [34]. Furthermore, when comparing the two catalysts, it is observed that the Ni-Cr catalyst was more active in promoting both reactions, which is explained by the higher amounts of the gases CO_2 and H_2; this outcome can be attributed to the higher Ni loading present, as well as a possible synergistic effect between the Ni and Cr [35,36].

For the process under hydrogen atmosphere (Figure 1B) and setting the non-catalytic hydropyrolysis process as a control, it was observed that both catalysts tested promoted higher CO and CH_4 formation, while CO_2 production remained significantly unchanged, which might suggest a possible inhibition of decarboxylation reactions. However, under a hydrogen atmosphere, nickel-based catalysts are well known to be selective in promoting hydrogenation reactions of CO_2 to form CH_4, with CO and H_2O constituting the main byproducts of this process [37]. Pieta et al. [38], while evaluating the efficiency of Ni-based catalysts in the reaction of hydrogenation of CO_2 to methane, showed that the tested catalysts were able to produce CH_4 with a yield of ≈97%, evidencing the high efficiency of these catalysts in the said process. Therefore, we suggest that, by the action of the catalysts, the CO_2 produced during the decarboxylation reactions was subsequently converted into CO and CH_4, keeping the yield of CO_2 close to that obtained in non-catalytic hydropyrolysis. In the Ni/SiO_2-catalyzed process, the yield of CO and CH_4 was increased by 20% and 770%, respectively. This compared to the non-catalyzed process, which produced 2.92 mol $kg_{SCB}{}^{-1}$ of CO and 0.05 mol $kg_{SCB}{}^{-1}$ of CH_4. When the Ni-Cr catalyst was added, the production of these gases increased by 30% for CO and 2070% for CH_4. The highest CH_4 production was observed in the process catalyzed by Ni-Cr, which, due to its higher Ni content, showed higher activity in the CO_2 hydrogenation process [38].

2.3. Influence of the Processes on the Composition of the Liquid Products

2.3.1. Chemical Characterization of Volatilizable Compounds by GC/MS

Through GC/MS analyses, between 102 and 125 compounds were detected in the LLFs produced in non-catalytic and catalytic pyrolysis under different reaction atmospheres. In total, about 55 to 64 chemical species were identified in the samples, resulting in the characterization of ≈80% of the total area of the total ion current chromatograms (TICCs). The identified compounds were grouped into different classes according to their main organic functions, these being divided into alcohols, sugar derivatives, alkylphenols, methoxyphenols, hydroxyphenols, phenols, carboxylic acids, nitrogenous, and furans. The chemical distribution of these compounds is shown in the class histograms.

From Figure 2, it is observed that all LLFs exhibited the same majority classes, which were as follows: alcohols, sugar derivatives, and phenolic compounds. Evaluating the effect of the atmosphere alteration, it was observed that the LLFs produced in the pyrolysis under inert atmosphere and hydropyrolysis process showed similar compositions (Figure S3 of the Supplementary Materials). The main difference is related to the relative content of sugar derivatives and alcohols. Under the H_2 atmosphere process, there was a higher proportion of sugar-derived molecules, whereas under the inert atmosphere process, the alcohols had a higher relative content. We propose, for this result, that the H_2 in the non-catalytic hydropyrolysis process provided a better stabilization of the radicals formed during the cracking of the biomass macromolecules (cellulose, hemicellulose, and lignin) [39]. As a result of the stabilization of the sugar derivatives (formed mainly from the thermal decomposition of cellulose), a restriction on the occurrence of secondary reactions was promoted during the process, resulting in the partial inhibition of the secondary reactions of cleavage and dehydration of these molecules to form alcohols.

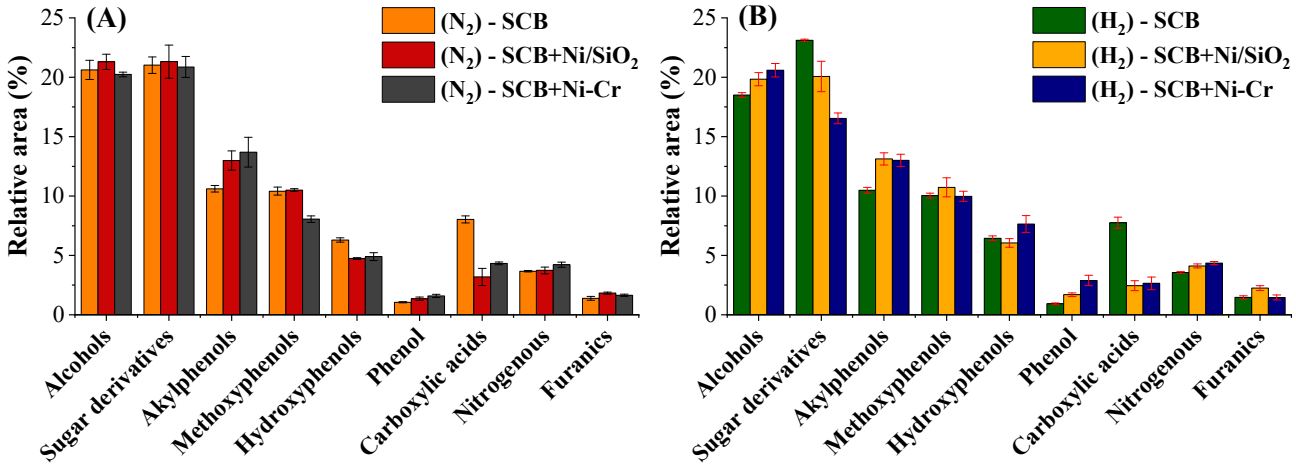

Figure 2. Histogram of classes of LLFs produced by (**A**) non-catalytic and catalytic pyrolysis, and (**B**) non-catalytic and catalytic hydropyrolysis.

Assessing the influence of catalysts under inert atmosphere (Figure 2A) and adopting the non-catalytic pyrolysis experiment as a control, it was noticed that the addition of catalysts in the reaction system promoted an increase in the relative area of alkylphenols and phenol, as well as a reduction in the percentage of hydroxyphenol- and carboxylic acid-type compounds. The percentages of alkylphenols and phenol in LLF from the non-catalytic process amounted to ≈11 and 1%, respectively. With the use of the Ni/SiO_2 catalyst, an increase of 22% in the alkylphenol content and 28% in the phenol content was achieved. These values were even higher when the Ni-Cr catalyst was used, for which increases of 28 and 50% were determined in the areas of alkylphenols and phenol, respectively. With respect to hydroxyphenols, the addition of catalysts promoted a reduction of ≈24% in the percentage of this class of compounds, when compared to the LLF produced in non-catalytic pyrolysis, where a relative content of 6.29% of hydroxyphenol molecules was

identified. Regarding carboxylic acids, it was observed that in the LLF produced in the non-catalytic process, the relative content of these species was ≈8%, and when Ni/SiO_2 and Ni-Cr catalysts were inserted into the process, the relative area of carboxylic acids was reduced by factors of ≈60 and 46%, respectively.

The reduction in the percentage area of hydroxyphenols and increase in phenol and alkylphenols suggests that the catalysts were active in promoting the partial dehydration of hydroxyphenols, producing the phenol compound, and subsequently, through alkylation reactions, the catalysts induced the formation of alkylated phenolics [40]. The reduction in the relative content of carboxylic acids, on the other hand, was caused by the activity of the catalysts in promoting decarboxylation reactions, since a higher production of CO_2 was found in the gaseous products that resulted from the catalytic processes. The production of phenolics from carboxylic acids can occur via radical reactions with the insertion of hydroxyl radicals ($OH^{\bullet}$) into the decarboxylated molecule, followed by aromatization to produce phenol, which leads to increased H_2 production in the gases, and alkylation mechanisms can also occur, inducing the formation of compounds of the alkylphenol class [34]. Another hypothesis to explain the production of alkylphenols from acids relates the decarboxylation reaction of lignin-derived acid species such as *p*-coumaric acid, producing alkylphenols such as 4-vinylphenol [41].

Evaluating the processes under H_2 atmosphere (Figure 2B), and setting the non-catalytic hydropyrolysis process as control, it was observed that the addition of catalysts to the process resulted in a decrease in the relative content of carboxylic acids and sugar derivatives, promoting an increase in the percentage of alcohols and phenolic compounds of the alkylphenol and phenol type. Regarding the acids, the percentage of this class of compounds in the LLF produced from the non-catalytic hydropyrolysis process amounted for 8%. Similarly to what was observed in the inert atmosphere processes, the addition of the catalysts promoted a ≈65% reduction in the content of acids present in both LLFs coming from the catalytic hydropyrolysis processes, proving that, in the H_2 atmosphere, the catalysts also have activity to promote decarboxylation reactions forming CO_2, which was subsequently converted to CO and CH_4 from its reduction and hydrogenation, respectively [37,38], as discussed in Section 2.2.

Regarding the sugar derivatives, in the catalytic processes under the H_2 atmosphere, it was observed that the catalysts promoted a reduction in the relative area of the compounds of this class. In non-catalytic hydropyrolysis, the relative area of the compounds of the sugar derivatives classes amounted to ≈23% of the total chromatogram area. Whereas in the Ni/SiO_2 and Ni-Cr catalyzed processes, the relative content of this class of compounds was reduced by ≈13 and 28%, respectively. Furthermore, in the catalyzed processes, there was an enhancement in the relative area of compounds of the class of alcohols, alkylphenols, and phenol monomer. In the LLF produced via non-catalytic hydropyrolysis, the relative area of these classes was equivalent to 18.50% for alcohols, 10.47% for alkylphenols, and 0.97% for phenols. In the process catalyzed by Ni/SiO_2, an increase of ≈7% in the relative content of alcohols, ≈24% in the percentage of alkylphenols, and ≈81% in the relative area of the phenol compound was observed. In the process using the Ni-Cr catalyst, there were increases of ≈11, ≈28, and ≈225% in the percentage of alcohols, alkylphenols, and phenols, respectively. A possible explanation for the conversion of sugar derivatives to alcohols and phenols relates the dehydration process of sugars to form oligomeric furan structures (pyrolytic humins) [42], which, in the presence of acid catalysts, and through alkylation, decarbonylation, and decarboxylation reactions can subsequently be converted to alcohols and phenols [43,44]. Furthermore, the largest changes were observed when the Ni-Cr catalyst was used, hence being more active for sugar conversion, an activity that may stem from the higher Ni content as well as the synergistic effect of the Cr present in the catalyst [45].

Another hypothesis to explain the increase in phenols relates to the occurrence of active radical stabilization in the catalyzed processes, since nickel, under H_2 atmosphere, promotes the division of molecular hydrogen into active atomic hydrogen species, forming

radicals ($H^{\bullet}$), increasing the reactivity of the reaction system [20,46]. On this basis, we propose that in the processes with the action of the catalysts, the major production of the phenol compound comes from radical reactions between the phenoxyl radical, which comes from the cracking of the biomass constituents and/or secondary cleavage of the vapors, with the hydrogen radical, which is believed to be present in greater availability in the reaction media. Moreover, since in the process using the Ni-Cr catalyst, this increase in phenol content was more significant, we suggest that the greater amount of Ni present in the catalyst has promoted greater activation of hydrogen available in the system, and consequently an enhanced reactivity during the process catalyzed by Ni-Cr [47].

For both processes, either in an inert or reactive atmosphere, the use of catalysts promoted the production of a bio-oil with a lower percentage of acidic species and higher relative content of phenolic monomers. However, under a reactive atmosphere, a higher catalytic activity was evidenced, which is explained by the higher reactivity of Ni in the presence of H_2 [20]. In this process, the catalysts used, principally the Ni-Cr catalyst, through the conversion of sugars and carboxylic acids, were more selective to produce a less oxygenated and more stable bio-oil, as well as with a higher content of phenolic species, mainly compounds of the alkylphenol and phenol monomer type, which have a high potential to serve as an alternative to petroleum-based phenols in applications such as non-ionic surfactants, antioxidant additives for the fuel industry, phenolic resins, and agrochemical products, and are thus compounds of high value and industrial application [27,46].

2.3.2. Molecular Characterization of Polar Compounds by UHRMS

Bio-oil is a complex, highly functionalized mixture with a high oxygen content, which makes it a highly polar matrix. This high polarity is one of the factors that limit the use of GC-based techniques in the characterization of bio-oils, which in turn are only capable of analyzing volatilizable components at operating temperature. In this context, to characterize the semi-volatile and non-volatile polar species present in the produced LLFs, ultra-high resolution mass spectrometry (UHRMS) technology, specifically HESI(±)-FT-Orbitrap MS, was used. The recent use of (UHRMS) has allowed for the assignment of molecular formulas to thousands of detected ions with high accuracy (error < 5 ppm), which enabled the characterization of samples at the molecular level, and hence made it possible to evaluate the effect of variables in the pyrolysis process [48] and catalytic processes [49], and more recently, we applied UHRMS to evaluate the influence of scale-up and reactor configuration on the chemical composition of cattle manure bio-oil [50].

Regarding UHRMS analysis, the use of electrospray ionization source (ESI) is the most widely adopted in the analysis of pyrolytic oils [51]. Thus, considering the high polarity of compounds present in bio-oils, ESI was used, as it allows a higher sensitivity for ionization of medium to high polarity species, for example, sugars and basic species, ionized mainly in the positive mode of ionization through the formation of $[M+Na]^+$ and $[M+H]^+$ type ions, and phenolic compounds and acidic species, ionized in the negative mode of ionization through the formation of $[M-H]^-$ [52,53]. From the analysis by UHRMS, the ionized compounds that had their molecular formula assigned were grouped into chemical classes according to the number of heteroatoms and analyzed using van Krevelen diagrams for speciation of possible reaction routes occurring in non-catalytic and catalytic pyrolysis and hydropyrolysis processes [54,55].

Negative-Mode (HESI(−)-FT-Orbitrap MS)

From the analyses of the LLFs by HESI(−)-FT-Orbitrap MS, between 2830 and 3173 ions were detected, of which molecular formulas were assigned to 1678–1870 species, resulting in an assignment of ≈60% of the ions detected in the LLFs. After processing the data, the results obtained were organized into class histograms (Figure 3).

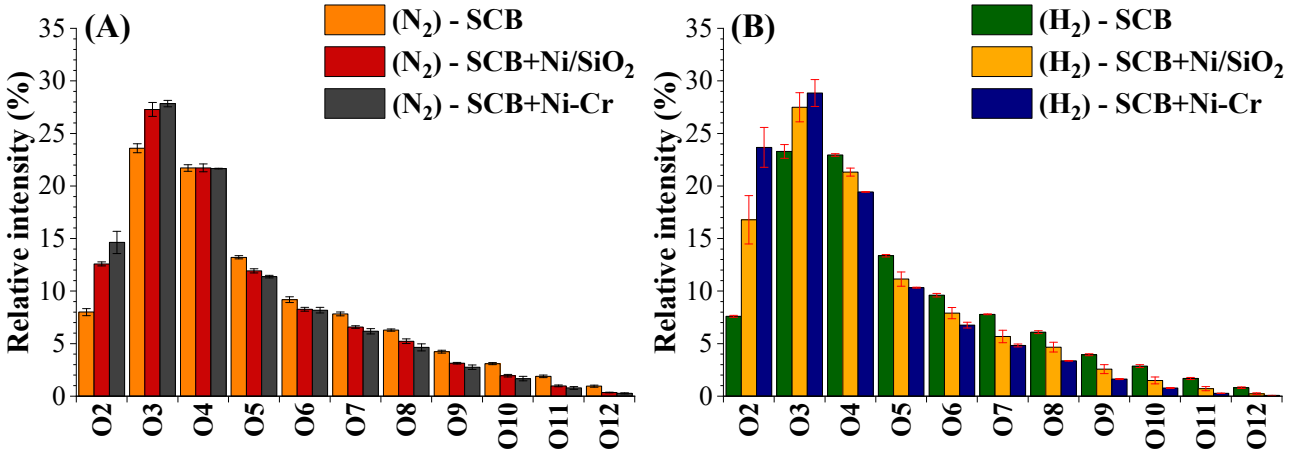

Figure 3. Histograms of classes of the LLFs produced by the processes in (**A**) inert atmosphere and (**B**) reactive atmosphere, analyzed by HESI(−)-FT-Orbitrap MS.

As shown in Figure 3, it was observed that all LLFs presented only classes of oxygenated compounds, containing from 2 to 12 oxygen atoms in their structure. Among these, the $O_{2–5}$ classes were the majority in all samples. Evaluating the effect of atmosphere alteration on the acidic polar compounds, it was observed that LLFs produced in the pyrolysis (N_2) and hydropyrolysis (H_2) process showed a similar class distribution, with no significant variations in class intensities (a comparison of these processes is available in Figure S5 of the Supplementary Materials). This result corroborates what was observed throughout this study, in which only the change of atmosphere from N_2 to H_2, under low pressures, does not exert a strong influence on the thermal conversion process, and therefore the products will have similar compositions [25].

When the effects of the use of catalysts were evaluated, it was observed that both catalysts (Ni/SiO_2 and Ni-Cr), under inert atmosphere, promoted a reduction in the intensity of the most oxygenated classes ($O_{5–12}$) and an increase in the classes of compounds with low oxygen content, containing two and three oxygen atoms in their structure. Summing the relative intensity of the O_5 to O_{12} classes, a value of ≈47% was obtained in the LLF of pyrolysis, while the Ni/SiO_2-catalyzed process reduced this value by a factor of ≈18%, and the Ni-Cr catalyzed process, by ≈23%. For O_2 and O_3 classes, the sum of the relative intensities resulted in 31.60% in LLF for the non-catalytic process, and when using Ni/SiO_2 and Ni-Cr catalysts in the process, this value was increased by factors of ≈26 and ≈35%, respectively, indicating that compounds with higher amounts of O are converted into less oxygenated species. Furthermore, the largest changes were exhibited in the Ni-Cr catalyzed process, corroborating the discussion regarding the higher activity of this catalyst, attributed to its higher Ni content when compared to the Ni/SiO_2 catalyst.

In the LLFs produced under the H_2 atmosphere, it was observed a reduction in the intensity of the species containing 4 to 12 oxygen atoms in their structure, and an increase in the intensity of the O_2 and O_3 classes. In the non-catalytic hydropyrolysis the $O_{4–12}$ classes, altogether, showed a relative intensity of 69%. This value was reduced by ≈20% and ≈31% when Ni/SiO_2 and Ni-Cr catalysts were used, respectively. Concerning classes O_2 and O_3, when combined they presented a relative intensity of ≈31% in the non-catalytic process. With the addition of Ni/SiO_2 and Ni-Cr catalysts, the relative intensity of these classes increased by factors of ≈43 and 70%, respectively. This result is corroborated by the higher reactivity of Ni in the hydrogen atmosphere, which in turn promoted a higher degree of conversion of more oxygenated molecules into species with a lower oxygen content [20,46].

The visualization of the data obtained via UHRMS in the van Krevelen diagram is an effective way to identify possible reaction mechanisms [56]. The slopes and intercepts of the lines in the van Krevelen diagrams and the shift of the intensities of the compounds in the regions established by the atomic ratios (H/C and O/C) can be visually associated with

cracking reactions and/or addition and/or removal of certain functional groups such as H_2O, CO_2, CO, CH_4, and H_2 [55]. The van Krevelen diagrams of H/C vs. O/C constructed for all classes found in LLFs are presented in Figure 4.

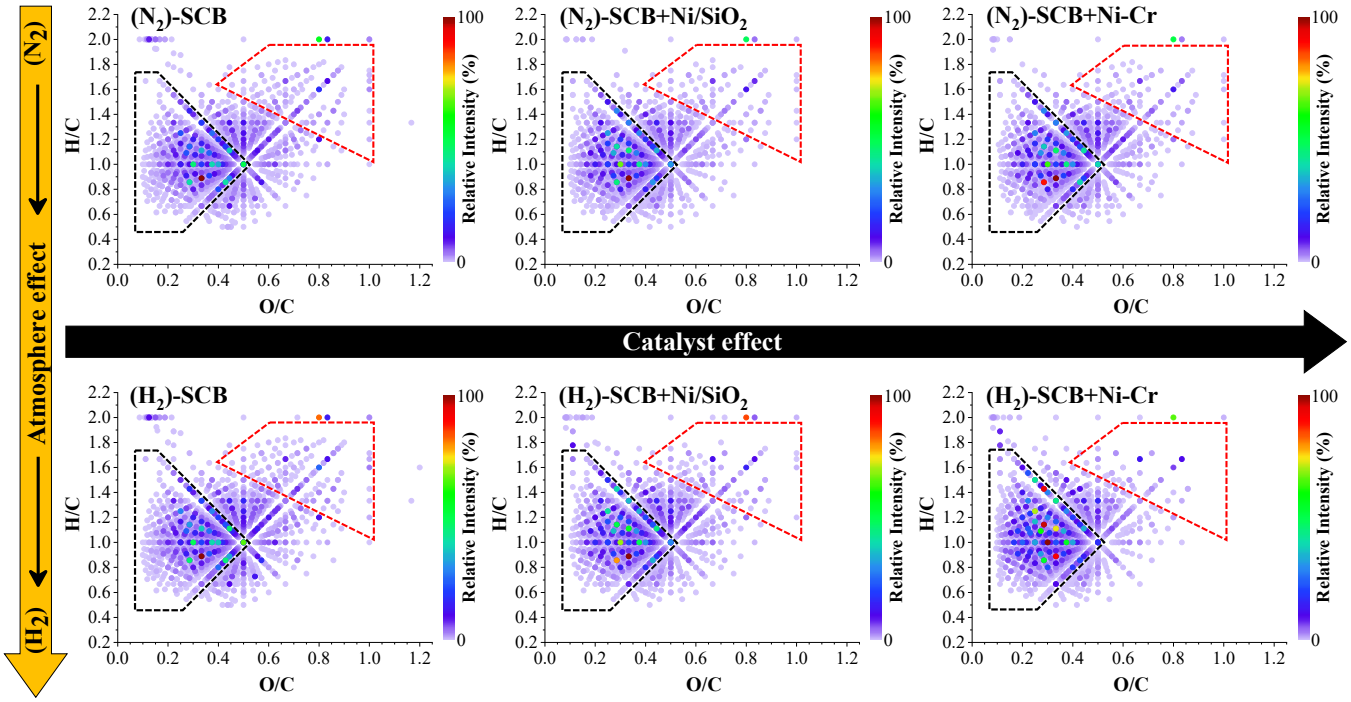

Figure 4. Van Krevelen diagrams for all classes of oxygenated compounds analyzed by HESI(−)-FT-Orbitrap MS.

On the basis of the analysis of van Krevelen diagrams, it was observed that the produced LLFs showed a higher content of compounds located in the region of H/C = 0.5–1.8 and O/C = 0.1–1.0. The modification of the atmosphere did not change the molecular profile of the samples obtained in the non-catalytic pyrolysis and hydropyrolysis processes. However, when evaluating the catalytic processes, it was observed that the catalysts promoted a reduction of the species present in the region of H/C ratio > 1.4 and O/C > 0.5 (area highlighted in red in Figure 4), which includes the region characteristic of compounds derived from sugars [49] and promoted an increase in the intensities of compounds in the range of H/C = 0.8–1.4 and O/C < 0.5 (area highlighted in black), which englobes the region of phenolic compounds [57]. For the pyrolysis under an inert atmosphere, the largest changes were evidenced when the Ni-Cr catalyst was used, and this result remains the same for the process under reactive atmosphere. However, when comparing the activity of the same catalysts in the different atmospheres, it was observed that in the presence of H_2, there was an enhanced catalytic activity, which can be seen by the greater changes in the molecular profile of the samples.

The decrease of compounds in the region of higher H/C and O/C ratios, characteristic of sugar derivatives, and the increase in the intensity of compounds present in the region attributed to phenolic compounds by Reymond et al. [57], corroborates the results obtained from the analyses of LLFs by GC/MS, where an increase in the relative area of phenolics and a reduction of sugar-derived species was observed. We suggest that this result is characteristic of dehydration reactions of sugar derivatives to form pyrolytic humins (a reaction that can be explained by the reduction of H/C and O/C following a diagonal trend [55]), which then undergo alkylation, decarbonylation, and decarboxylation, producing phenolic compounds [42,43]. The result of dehydration of sugar derivatives in the catalytic processes and formation of humin structures can be best visualized from the analysis of LLFs using

HESI ionization in the positive mode, since it is the most suitable ionization mode for analysis of these species [49].

Positive-Mode (HESI(+)-FT-Orbitrap MS)

Between 4381 and 5923 ions were detected in the analyses of LLFs by HESI(+)-FT-Orbitrap MS, of which molecular formula 2566–2965 species were assigned, resulting in an assignment of 46 to 62% of the ions detected in the LLFs produced by the different processes. After processing the data, the results obtained were sorted into histograms of classes and are available in Figure 5.

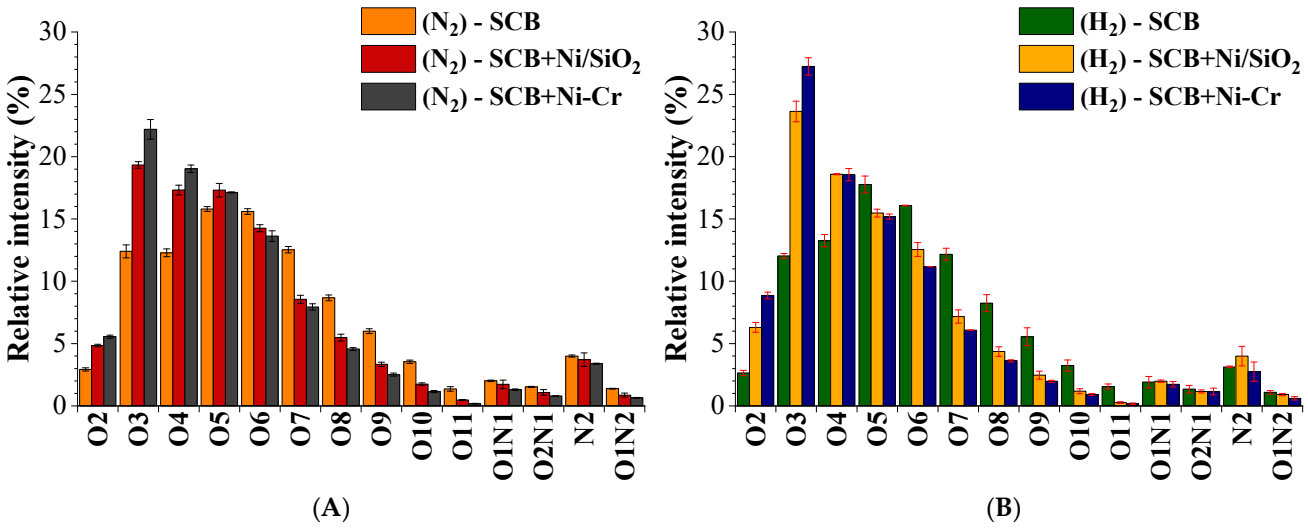

Figure 5. Histograms of classes of the LLFs produced by the processes in (**A**) inert atmosphere and (**B**) reactive atmosphere, analyzed by HESI(+)-FT-Orbitrap MS.

The LLF samples exhibited the same classes of compounds, which contain mainly O_x-type species (x = 2–11), and, in smaller proportions, nitrogen species of the classes O_1N_1, O_2N_1, O_1N_2, and N_2. Regarding the composition in terms of the class distribution of the LLFs produced in the pyrolysis and non-catalytic hydropyrolysis processes, it was confirmed, as well as in the quantitative and qualitative analyses of the products obtained by these processes, that there was a low influence of the atmosphere on the compounds analyzed in the positive mode (the comparison between the samples is available in Figure S6 of the Supplementary Materials). However, when adding the catalysts to the process, the tendency to convert the more oxygenated molecules into species with a lower oxygen content was noticed (Figure 5). The $O_{2–4}$ grades had their relative intensities increased with the addition of the catalysts to the process, while the classes with higher oxygen content molecules ($O_{6–11}$) had their relative intensities reduced. For the nitrogen classes, no changes were observed.

Regarding pyrolysis under inert atmosphere and adopting the non-catalytic process as a control, it was observed that the intensity of classes $O_{6–11}$ (≈48% in the non-catalytic process) reduced by ≈29 and 37% when using the Ni/SiO_2 and Ni-Cr catalysts, respectively. In the LLF produced from non-catalytic pyrolysis, the intensity of the summed $O_{2–4}$ classes was 26.71%., while when the Ni/SiO_2 catalyst was used in the process, the intensity of the compounds of these classes increased by ≈50%. In addition, in the Ni-Cr-catalyzed process, the intensities of $O_{2–4}$ classes increased by a factor of 69%. More significant results were observed in the H_2 atmosphere process. In this process, the Ni/SiO_2 and Ni-Cr catalysts promoted increases of ≈74 and 96% in the intensity of classes $O_{2–4}$, compared to the non-catalyzed process, in which these classes, when added together, presented relative intensity of ≈28%. Aligned with the formation of less oxygenated molecules is the reduction of more oxygenated structures. In the non-catalytic process, the intensity of the classes containing 5 to 11 oxygen atoms in their structure was ≈47%. Conversely, when

using the Ni/SiO_2 and Ni-Cr catalysts, the intensity of these classes was reduced by factors of ≈40 and 49%, respectively.

To confirm the hypotheses raised about the activity of catalysts in promoting dehydration mechanisms of sugars, van Krevelen diagrams of H/C vs. O/C were constructed for the $O_{2–11}$ classes of compounds present in the LLFs, available in Figure 6.

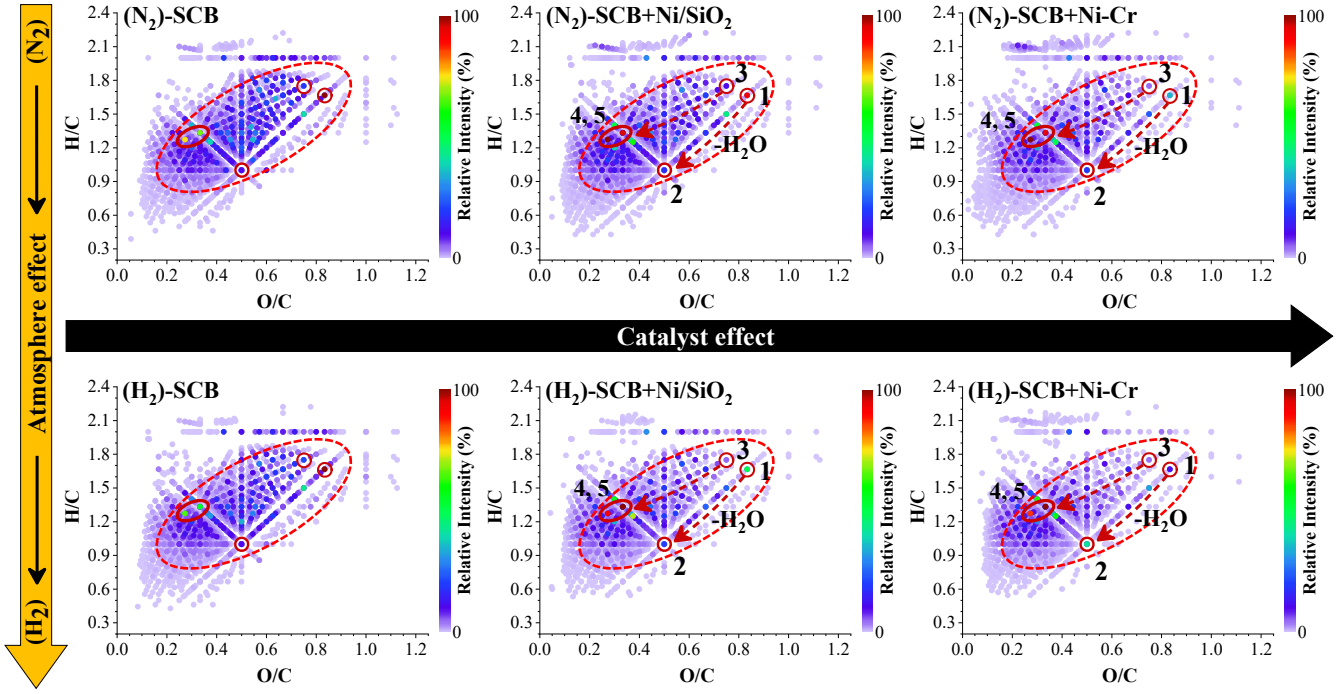

Figure 6. van Krevelen diagrams for the classes of Ox-type compounds (x = 2–11) analyzed by HESI(+)-FT-Orbitrap MS.

For all LLFs, the oxygenated compounds are most abundantly distributed in the region of H/C ≥ 1 and O/C between 0.1 and 1 in the van Krevelen plots. The profile plots of the samples produced from the non-catalytic processes showed that the molecular distribution of the compounds did not change in terms of atomic ratios. With respect to the catalytic processes, it was observed that the catalysts acted to reduce the relative intensities of the compounds located mainly in the range H/C > 1.0 and O/C = 0.1–1.0 (region demarcated in the diagram). The largest changes occurred in sugar derivatives at H/C > 1.5 and O/C > 0.6 [49], which was most evident in processes under the H_2 atmosphere, especially in the Ni-Cr-catalyzed process.

The results of the analyses of LLFs in the positive mode suggest routes of conversion of sugars into molecules with H/C ratios = 1.0–1.5 and O/C = 0.1–0.5, characteristic of pyrolytic humin structures, which are products of the dehydration of sugar structures [42,56]. As an example, we can consider the dehydration of the molecules highlighted in the diagrams in Figure 6, where molecule 1 ($C_6H_{10}O_5$) undergoes dehydration, resulting in the formation of molecule 2 ($C_6H_6O_3$), as well as molecule 3 ($C_8H_{14}O_6$), which can be dehydrated and after complementary reactions form compound 4 ($C_9H_{12}O_3$) and 5 ($C_{11}H_{14}O_3$). The proposed structures for these molecular formulas are shown in Figure 7, schemes 1 and 2, respectively. Zhang et al. [43] describes that these dehydrated structures can undergo alkylation, decarbonylation, and decarboxylation reactions, yielding phenolics, which is corroborated by the data from the characterizations of the liquid fractions by GC/MS and by HESI(−)-FT-Orbitrap MS.

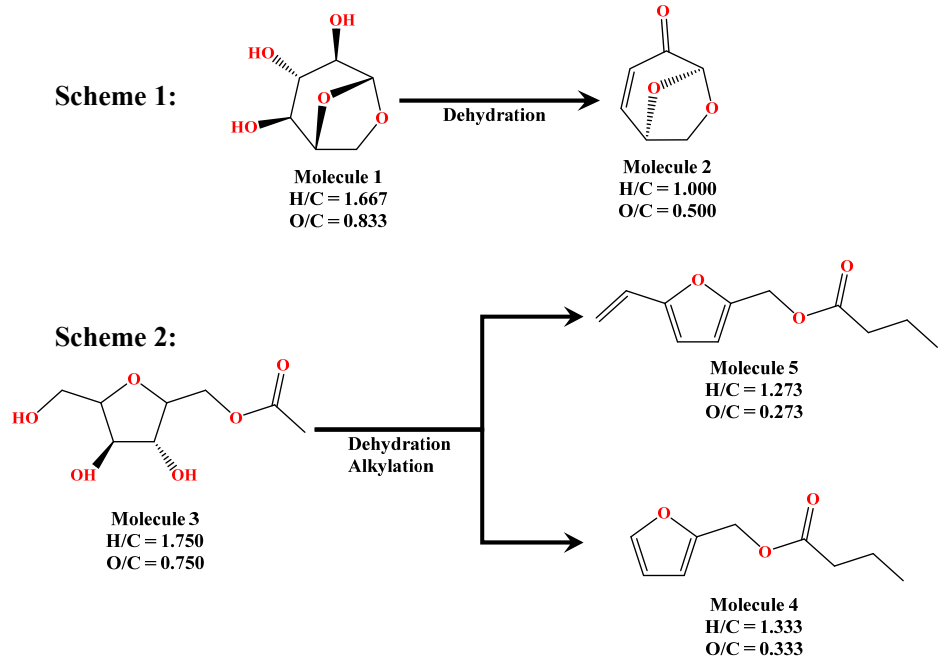

Figure 7. Conversion routes for the proposed structures for molecules 1, 2, 3, 4, and 5.

Through the dataset obtained from the characterization of LLFs by UHRMS, it was possible to obtain relevant knowledge about the activity of catalysts under an inert or reactive atmosphere. In both processes, the use of Ni/SiO_2 and Ni-Cr catalysts in the thermal conversion process promotes the deoxygenation of bio-oil through the conversion of more oxygenated compounds into species with lower oxygen content, and with similar reaction mechanisms. From the analysis of van Krevelen diagrams, it was observed that, regardless of the atmosphere, the catalysts are active in the conversion of species with higher H/C and O/C ratios, such as sugar derivatives, into less oxygenated and aromatic compounds, such as the phenolics, acting mainly by dehydration reactions, although in the hydropyrolysis process, a greater degree of deoxygenation was evidenced due to the greater reactivity of Ni in the H_2 atmosphere, as previously mentioned. Even though the catalysts showed similar reaction mechanisms, the Ni-Cr was the most active in deoxygenating the bio-oil, which may be the effect of a higher nickel loading, as well as due to the presence of chromium in its composition. By correlating the results of the analysis by UHRMS with the data from the characterization of LLFs by GC/MS and of gases by uGC-TCD, it was observed that the catalysts were active mainly in the dehydration of molecules derived from sugars and, through other mechanisms reactions, such as decarboxylation, decarbonylation, and alkylation, were selective for the production of phenolic species, increasing the content of these compounds in the bio-oil and, consequently, increasing the potential of using the product as an industrial raw material and a renewable source of chemical inputs of high added value, allowing greater economic return for the sugar-energy industries.

3. Materials and Methods

3.1. Materials

The sugarcane bagasse was collected at the sugarcane biorefinery, located in Iracemápolis, São Paulo, Brazil. After collection, the biomass was air-dried to reduce the residual moisture of the sample to a content below 10%. After the drying period, the SCB was subjected to a milling process using an SK100 transverse beater mill to produce particles $\leq$ 2 mm. Next, the SCB was subjected to immediate and elemental analyses. The procedure and results of the biomass characterization analyses are available in the feedstock characterization section of the Supplementary Materials.

3.2. Experimental Procedure

3.2.1. Micro-Scale Non-Catalytic and Hydropyrolysis Experiments

As previously mentioned, the catalytic and non-catalytic pyrolysis and hydropyroly-sis experiments were performed under atmospheric pressure, using a microreactor constituted of two connected furnaces, where the first operated at 500 °C and the second at 350 °C. In each of the furnaces, a heating element was connected to temperature controllers for heating the system. The reactor section consists of a borosilicate glass tube (500 × 4 mm) crossing for the two furnaces. Nitrogen (N_2) or hydrogen (H_2) were introduced in the initial section of the pyrolysis reactor. On the other reactor side, at the exit of pyrolysis vapors, a cartridge containing activated carbon and glass wool was arranged, functioning as a trap to capture the produced bio-oil. The microreactor layout is illustrated in Figure 8.

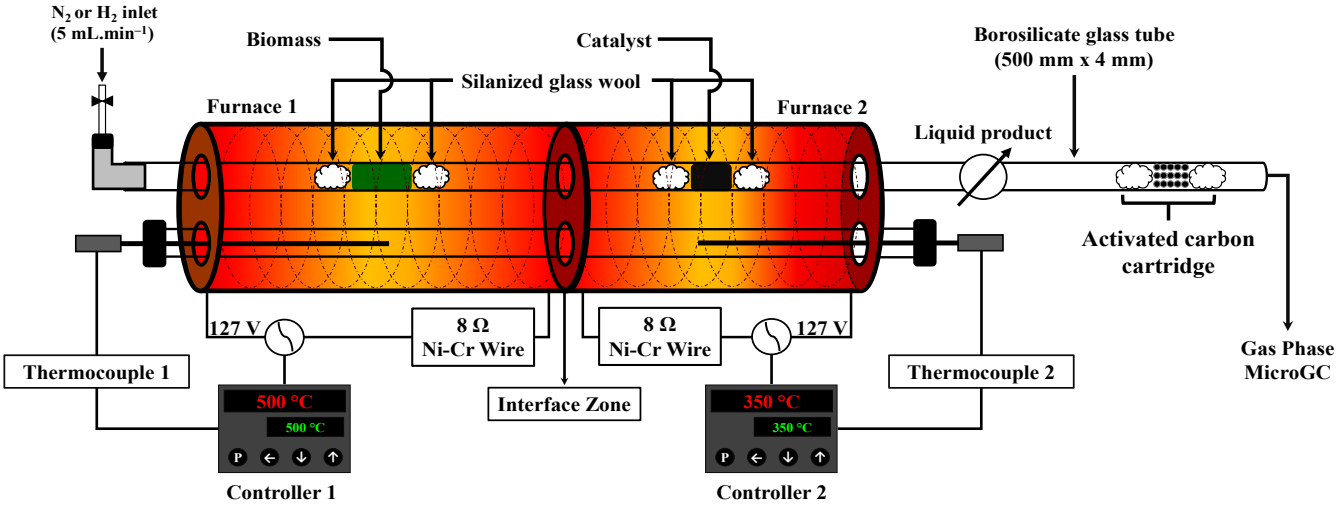

Figure 8. Micro-scale pyrolysis reactor.

Approximately 50 mg of SCB and 25 mg of catalyst were introduced inside the tube, both supported with glass wool, as shown in Figure 8. After the mass weighing step, the tube was inserted into the heating system, and before the experiment, for total oxygen removal, the tube was purged for 2 min using the gas responsible for the reaction atmosphere under a flow rate of 5 mL min^{-1}, which was kept the same throughout the process. Then, the furnace 2 was heated up to a temperature of 350 °C. After this procedure, concomitant with the beginning of the experiment, furnace 1 was heated at a rate of ≈250 °C min^{-1} until it reached a temperature of 500 °C, and it was kept at this temperature for 30 s. Afterwards, the system was turned off and cooled down to room temperature with the support of a cooler fan. It is worth mentioning that during the entire process, the gaseous product formed was collected in sample bags and analyzed immediately using an Agilent 490 Micro-GC Biogas Analyzer system.

When the reactor reached room temperature, the fraction of chemical compounds that condensed after the catalyst bed at the outlet of the second furnace, named light liquid fraction (LLF), was eluted with the solvent tetrahydrofuran (THF), previously distilled, and collected in a volumetric flask with a capacity of 5 mL. The volume was transferred to an amber flask for storage and further analysis. The heavy liquid fraction (HLF), the portion that condensed in the interface between the two furnaces (Figure 8), with a temperature zone between 500 and 350 °C, was eluted with THF. The solvent was then evaporated at room temperature and subsequently had its mass measured for mass balances. The explanation about the fractionation of the total liquid product into LLF and HLF, as well as the detailed procedure for recovery of the products separately, is available in the LLF and HLF recovery process section of the Supplementary Materials. To facilitate the reading and interpretation of the data, each process performed was identified according to the following

nomenclature code: (Atmosphere) − SCB + Catalyst. To minimize the influence of random errors, all the processes described here were performed in triplicate.

3.2.2. Gravimetric Yields

Prior to each experiment, the mass of the reactor containing the biomass and catalyst was measured, and on the basis of this, the yield of non-condensable gases was determined through the difference of the mass of the tube before and after the thermochemical conversion process, as shown in Equation (1).

$$Y_{Gases} = \left(\frac{M_i - M_f}{M_{SCB}}\right) \times 100 \quad (1)$$

where the terms M_i and M_f correspond to the mass of the reactor before and after the pyrolysis process, respectively, and M_{SCB} is the mass of biomass used. After the gravimetric determination of the gases, the reactor was washed with solvent to recover the liquid product (LLF + HLF), and then, to evaporate the solvent residue, the reactor was left to stand for 24 h. After this period, the biochar was removed from inside the reactor and had its mass measured. The yield was determined according to Equation (2).

$$Y_{Biochar} = \left(\frac{M_{Bc}}{M_{SCB}}\right) \times 100 \quad (2)$$

where the term M_{Bc} refers to the mass of biochar. The liquid product produced was separated into light and heavy fractions. The heavy fraction was eluted with THF and collected in a 2 mL flask of known mass. The solvent was then evaporated at room temperature, and its mass was subsequently measured. Its yield was calculated according to Equation (3).

$$Y_{HLF} = \left(\frac{M_v - M_{vs}}{M_{SCB}}\right) \times 100 \quad (3)$$

where the terms M_v and M_{vs} correspond to the mass of the flask without sample and with the sample after evaporation of the solvent, respectively. The yield of the light liquid fraction was determined by difference, as described by Equation (4).

$$Y_{LLF} = 100 - (Y_{Gases} + Y_{Biochar} + Y_{HLF}) \quad (4)$$

3.3. Analytical Methods

3.3.1. Biochar Characterization

Elemental analysis of the biochar samples obtained during the thermal and catalytic processes was performed using a LECO CHN628 elemental analyzer, and the results were treated in LECO CHN628 Software ver. 1.30 (St. Joseph, MI, USA). The equipment was operated with helium (99.995%) and oxygen (99.99%), with furnace temperature at 950 °C and post-firing temperature at 850 °C. Other parameters were adjusted for better sensitivity. The equipment was calibrated with an EDTA standard (41.0% C, 5.5% H, and 9.5% N) using a mass range between 10 and 200 mg. The samples were analyzed using 30.0 mg on tin foil. The ash content present in the biochar samples was estimated on the basis of the ash content present in the biomass, mass of biomass used in the thermal conversion process, and the biochar yield as shown in Equation (5).

$$Ash_{BC}(wt\%) = \frac{(Ash_{SCB} \times M_{SCB})}{(Y_{BC} \times M_{SCB})} = \frac{Ash_{SCB}}{Y_{BC}} \quad (5)$$

where Ash_{SCB} refers to the ash content present in the biomass and Y_{BC} corresponds to the obtained biochar yield.

3.3.2. Characterization of the Gaseous Products by μGC-TCD

Analysis and quantification of the gaseous products obtained from non-catalytic and catalytic pyrolysis and hydropyrolysis were performed using an Agilent 490 Micro-GC Biogas Analyzer (Santa Clara, CA, USA) system equipped with a thermal conductivity detector (TCD). The system consisted of a two-channel module, with a CP-Molsieve 5A column in the first channel and a CP-PoraPLOT U column in the second channel. Each column had a length of 10 m.

The hydrogen (H_2), oxygen (O_2), nitrogen (N_2), and carbon monoxide (CO) produced were quantified using the first column, with argon as the carrier gas. The second column was used for the quantification of CO_2 and CH_4, with helium as the mobile phase. A standard gas mixture consisting of H_2, N_2, CH_4, CO, CO_2, C_2H_6, C_2H_4, and C_3H_8 was used to calibrate the instrument for gas composition quantification. The operating conditions were as follows: injector temperature of 50 °C, with 50 ms injection; initial pressures of 25 and 20 psi in the first and second channels, respectively; oven temperatures of 70 and 50 °C in the first and second channels, respectively. The analysis time was 140 s.

3.3.3. Characterization of the Liquid Products by Gas Chromatographic/Mass Spectrometry (GC/MS)

The analysis of bio-oils by GC-based methods is usually performed directly, i.e., without including a process of prior treatment of the sample. However, this form of analysis does not allow good volatilization, nor sensitivity, for the analysis and detection of functionalized species such as phenols, carboxylic acids, sugar derivatives, and others present in large quantities in the bio-oil. To solve these problems and provide a better chemical characterization, the bio-oil needs to undergo a derivatization step [58,59]. Thus, the solutions containing the LLFs obtained from each of the thermal conversion processes were subjected to the derivatization process by silylation, employing N,O-bis(trimethylsilyl)trifluoroacetamide (BSTFA) as the derivatizing agent. First, 20 μL of the derivatizing agent was added to 60 μL of the solution containing the sample in THF. Then, the resulting solution was kept tightly closed and heated at 60 °C for 30 min. After this period, the samples were directed to gas chromatography/mass spectrometry (GC/MS) analysis.

Analysis of the produced LLFs was performed using a Thermo-Fisher Scientific model TRACE 1310/TSQ 9000 system (Thermo-Fisher Scientific, Austin, TX, USA) equipped with an NA-5MS column (60 m × 0.25 mm; 0.25 μm). The oven temperature was programmed as follows: 50 °C (2 min); 5 °C min^{-1} until 290 °C (maintained for 10 min). The carrier gas used was helium, at a constant flow rate of 1 mL min^{-1}. The injector was operated at 280 °C, in split mode (1:20), with an injection volume of 1 μL. The mass spectrometer was operated in electron ionization mode (70 eV), with scanning in the mass range (m/z) from 40 to 550 Da, and the interface temperature was 290 °C. The data were further processed using Chromeleon 7.2 software (Thermo Scientific, Sunnyvale, CA, USA), and compounds were identified by comparing the experimentally obtained spectra with the NIST 2017 spectral library databases ver. 2.73 (Gaithersburg, MD, USA), considering only those species for which the correspondence with the library spectra was greater than 75%.

3.3.4. Characterization of the Liquid Products by Heated Electrospray Ionization Coupled to a Fourier Transform Orbitrap Mass Spectrometer (HESI(±)-FT-Orbitrap MS)

LLF samples were prepared as follows: aliquots of 50 μL of the solutions containing the samples in THF were diluted in 950 μL of methanol to obtain final solutions of concentrations of 200 μg mL^{-1}. For UHRMS analysis in negative and positive ion modes, a Orbitrap Exactive Plus instrument (Thermo-Fisher Scientific, Bremen, Germany) equipped with an Ion Max API source with HESI-II probe was used. Mass spectra were acquired with a mass resolution of 140,000 FWHM (full width at half maximum) at m/z 200. For the negative ion mode, the conditions were as follows: sheath gas flow, 15 arbitrary units (AU); auxiliary gas flow, 5 AU; sweep gas flow, 2 AU; ion source temperature, 30 °C; capillary temperature, 320 °C; spray voltage, −4.0 kV; and scanning range, 100–700. For the positive

ion mode, the conditions were as follows: sheath gas flow, 25 AU; auxiliary gas flow, 0 AU; sweep gas flow, 0 AU; ion source temperature, 80 °C; capillary temperature, 320 °C; spray voltage, +3.8 kV; and scanning range, 100–700.

In both ionization modes, the final mass spectrum of each sample was obtained after subtraction of the mass spectrum of the blank. Data processing was performed using Xcalibur 3.0.63 software (Thermo-Fisher Scientific, Inc.). To ensure accurate assignment of molecular formulas, the composition constraints were adjusted to allow the assignment of isotopic formulas containing ^{12}C, ^{1}H, ^{16}O, ^{14}N, and ^{23}Na, and a tolerance error ≤ 3 ppm. The criteria for assigning the molecular formula to the ions detected in the negative mode were as follows: $^{12}C_{4–50}$, $^{1}H_{4–100}$, $^{14}N_{0–3}$, and $^{16}O_{0–15}$; double bond equivalent (DBE) 0–35; and charge −1. For the positive mode, on the other hand, the criteria were as follows: $^{12}C_{4–50}$, $^{1}H_{4–100}$, $^{14}N_{0–5}$, $^{16}O_{0–15}$, and $^{23}Na_{0–1}$; double bond equivalent (DBE) 0–35; and charge +1. After the elemental compositions were assigned, the data were transported to Microsoft Excel for consistency analysis of the molecular assignment, employing the criteria reported in [60], and construction of class histograms and contour plots, where only ions with relative intensity ≥ 0.01 were considered.

4. Conclusions

The results showed that the change of the reaction atmosphere in the non-catalytic thermal conversion process of sugarcane bagasse, under atmospheric pressure, did not affect the yields of the products obtained, as well as causing no change in the chemical compositions of pyrolytic products. Analyzing the influence of the use of catalysts in the processes, and comparing with the non-catalytic processes, increases of up to 31% in the yields of the gaseous products and reductions of up to 9% in the yields of LLFs obtained were observed, which is also reflected in the change in the chemical composition of these products. The largest changes were observed in the processes under the H_2 atmosphere, in which the Ni-based catalysts showed higher activity. Considering the catalytic experiments under hydrogen atmosphere, the influence of catalysts on the gaseous products occurred mainly through CO_2 hydrogenation mechanisms, promoting an increase of up to 2070 and 30% in the yields of CH_4 and CO gases, respectively, when compared to the non-catalytic process.

Regarding the chemical composition of the liquid products of the thermocatalytic conversion processes, the results showed that the catalysts were selective in the decarboxylation of carboxylic acids and the reduction of species derived from sugars, as well as promoting increased production of phenolic compounds, which was observed in the GC/MS analyses and corroborated by the UHRMS data, where the reduction of species containing 4–12 oxygen atoms, which are normally attributed to carbohydrate-type compounds, and increase of aromatic compounds containing 2–3 oxygen atoms, characteristic of phenolic structures, were observed. This is confirmed by the van Krevelen diagrams, which showed that the dehydration reaction of the sugars was the main reaction mechanism that occurred in the catalyzed processes, converting the sugar derivatives to pyrolytic humin structures, which, followed by secondary deoxygenation and alkylation reactions, were converted to phenolic compounds. When comparing the performance of the two catalysts, the catalyst with the higher Ni loading, Ni-Cr, showed higher activity for deoxygenation of the compounds, as well as producing a bio-oil with higher phenolic monomer content. In summary, the thermocatalytic conversion of sugarcane bagasse under H_2 atmosphere and in the presence of nickel-based catalysts presents a higher efficiency in the deoxygenation of pyrolytic vapors, acting selectively in the deoxygenation of carboxylic acids and sugar derivatives, through reactions of decarboxylation and dehydration, respectively, and promoting the enrichment of phenolic compounds in bio-oil, which have a wide industrial application and potential as substitutes for compounds derived from fossil sources.

Supplementary Materials: The following supporting information can be downloaded at: https://www.mdpi.com/article/10.3390/catal12040355/s1. Table S1. Biomass properties. Figure S1. LLF and HLF recovery process. Figure S2. Tukey post hoc statistical test from the analysis of variance (ANOVA) for each of the products: (A) LLF, (B) gases, (C) HLF, and (D) biochar. Figure S3. Tukey post hoc statistical test from analysis of variance (ANOVA) for each of the species present in the gases: (A) CO_2, (B) CO, (C) CH_4, and (D) H_2. Figure S4. Comparison of the volatilizable composition of LLFs produced in the non-catalytic processes. Figure S5. Comparison of the polar composition of LLFs produced in the non-catalytic processes, analyzed by HESI(−)-FT-Orbitrap MS. Figure S6. Comparison of the polar composition of LLFs produced in the non-catalytic processes, analyzed by HESI(+)-FT-Orbitrap MS.

Author Contributions: T.M.S.—investigation, instrumental analysis, interpretation of the results, writing—original draft; W.R.d.S.—interpretation of results, critical revision of the manuscript; J.d.C.C.—interpretation of results, critical revision of the manuscript; C.C.S.—selection of catalysts, interpretation of results, critical revision of the manuscript; R.M.—collection, preparation and biomass characterization; K.R.—conceptualization, final revision of the manuscript; N.D.—conceptualization, final revision of the manuscript; A.W.J.—project coordinator, resources, conceived and designed the analyses, data analysis, final revision of the manuscript. All authors have read and agreed to the published version of the manuscript.

Funding: This research received no external funding.

Acknowledgments: The authors from the PEB research group (UFS) are grateful to CAPES (Coordination of Improvement of Higher Educational Personal) and CNPq (Brazilian National Research Council) for fellowships and CLQM (Center of Multi-users Chemistry Laboratories, Federal University of Sergipe) for analytical assistance. The authors are grateful to GESP (São Paulo Government) for the financial support for the biomass characterization assistance carried out by the LBE (Laboratory of Bioenergy and Energy Efficiency) from IPT. The authors also thanks Karlsruhe Institute of Technology for the support to the institutional consortium KIT-UFS-IPT and KIT-Publication Fund.

Conflicts of Interest: The authors declare no conflict of interest.

References

1. Wang, P.; Zheng, Y.; Liang, X.; Jia, Z.; Wang, X.; Guo, Y.; Ren, L. Pyrolysis of sugarcane bagasse for bio-chemicals production catalyzed by micro-mesoporous composite molecular sieves. *Chem. Pap.* **2021**, *75*, 3283–3293. [CrossRef]
2. Nunes, V.O.; Fraga, A.C.; Silva, R.V.S.; Pontes, N.S.; Pinho, A.R.; Sousa-Aguiar, E.F.; Azevedo, D.A. Chemical characterisation of sugarcane bagasse bio-oils from hydrothermal liquefaction: Effect of reaction conditions on products distribution and composition. *J. Environ. Chem. Eng.* **2021**, *9*, 106513. [CrossRef]
3. Ajala, E.O.; Ighalo, J.O.; Ajala, M.A.; Adeniyi, A.G.; Ayanshola, A.M. Sugarcane bagasse: A biomass sufficiently applied for improving global energy, environment and economic sustainability. *Bioresour. Bioprocess.* **2021**, *8*, 87. [CrossRef]
4. CONAB-Companhia Nacional de Abastecimento Acompanhamento da Safra Brasileira de Cana-de-Açúcar. Available online: https://www.conab.gov.br/component/k2/item/download/38841_c46487b7985626b6b41f7083ce9336c5 (accessed on 27 December 2021).
5. Toscano Miranda, N.; Lopes Motta, I.; Maciel Filho, R.; Wolf Maciel, M.R. Sugarcane bagasse pyrolysis: A review of operating conditions and products properties. *Renew. Sustain. Energy Rev.* **2021**, *149*, 111394. [CrossRef]
6. Ordonez-Loza, J.; Chejne, F.; Jameel, A.G.A.; Telalovic, S.; Arrieta, A.A.; Sarathy, S.M. An investigation into the pyrolysis and oxidation of bio-oil from sugarcane bagasse: Kinetics and evolved gases using TGA-FTIR. *J. Environ. Chem. Eng.* **2021**, *9*, 106144. [CrossRef]
7. Schmitt, C.C.; Moreira, R.; Neves, R.C.; Richter, D.; Funke, A.; Raffelt, K.; Grunwaldt, J.-D.; Dahmen, N. From agriculture residue to upgraded product: The thermochemical conversion of sugarcane bagasse for fuel and chemical products. *Fuel Process. Technol.* **2020**, *197*, 106199. [CrossRef]
8. Suriapparao, D.V.; Vinu, R. Biomass waste conversion into value-added products via microwave-assisted Co-Pyrolysis platform. *Renew. Energy* **2021**, *170*, 400–409. [CrossRef]
9. Shirazi, Y.; Viamajala, S.; Varanasi, S. In situ and Ex situ Catalytic Pyrolysis of Microalgae and Integration with Pyrolytic Fractionation. *Front. Chem.* **2020**, *8*, 786. [CrossRef]
10. Li, Z.; Zhong, Z.; Yang, Q.; Ben, H.; Seufitelli, G.V.S.; Resende, F.L.P. Parametric study of catalytic hydropyrolysis of rice husk over a hierarchical micro-mesoporous composite catalyst for production of light alkanes, alkenes, and liquid aromatic hydrocarbons. *Fuel* **2022**, *310*, 122457. [CrossRef]
11. Lu, Q.; Zhang, Z.; Wang, X.; Guo, H.; Cui, M.; Yang, Y. Catalytic Fast Pyrolysis of Biomass Impregnated with Potassium Phosphate in a Hydrogen Atmosphere for the Production of Phenol and Activated Carbon. *Front. Chem.* **2018**, *6*, 32. [CrossRef]

12. Dyer, A.C.; Nahil, M.A.; Williams, P.T. Catalytic co-pyrolysis of biomass and waste plastics as a route to upgraded bio-oil. *J. Energy Inst.* **2021**, *97*, 27–36. [CrossRef]
13. Liang, J.; Shan, G.; Sun, Y. Catalytic fast pyrolysis of lignocellulosic biomass: Critical role of zeolite catalysts. *Renew. Sustain. Energy Rev.* **2021**, *139*, 110707. [CrossRef]
14. Stummann, M.Z.; Høj, M.; Gabrielsen, J.; Clausen, L.R.; Jensen, P.A.; Jensen, A.D. A perspective on catalytic hydropyrolysis of biomass. *Renew. Sustain. Energy Rev.* **2021**, *143*, 110960. [CrossRef]
15. Chen, X.; Che, Q.; Li, S.; Liu, Z.; Yang, H.; Chen, Y.; Wang, X.; Shao, J.; Chen, H. Recent developments in lignocellulosic biomass catalytic fast pyrolysis: Strategies for the optimization of bio-oil quality and yield. *Fuel Process. Technol.* **2019**, *196*, 106180. [CrossRef]
16. Dai, L.; Wang, Y.; Liu, Y.; He, C.; Ruan, R.; Yu, Z.; Jiang, L.; Zeng, Z.; Wu, Q. A review on selective production of value-added chemicals via catalytic pyrolysis of lignocellulosic biomass. *Sci. Total Environ.* **2020**, *749*, 142386. [CrossRef]
17. Aparecida da Silveira Rossi, R.; Barbosa, J.M.; Antonio de Souza Barrozo, M.; Martins Vieira, L.G. Solar assisted catalytic thermochemical processes: Pyrolysis and hydropyrolysis of Chlamydomonas reinhardtii microalgae. *Renew. Energy* **2021**, *170*, 669–682. [CrossRef]
18. Santana Junior, J.A.; Menezes, A.L.; Ataíde, C.H. Catalytic upgrading of fast hydropyrolysis vapors from industrial Kraft lignins using ZSM-5 zeolite and HY-340 niobic acid. *J. Anal. Appl. Pyrolysis* **2019**, *144*, 104720. [CrossRef]
19. Ding, Y.-L.; Wang, H.-Q.; Xiang, M.; Yu, P.; Li, R.-Q.; Ke, Q.-P. The Effect of Ni-ZSM-5 Catalysts on Catalytic Pyrolysis and Hydro-Pyrolysis of Biomass. *Front. Chem.* **2020**, *8*, 790. [CrossRef]
20. Hu, M.; Cui, B.; Xiao, B.; Luo, S.; Guo, D. Insight into the Ex Situ Catalytic Pyrolysis of Biomass over Char Supported Metals Catalyst: Syngas Production and Tar Decomposition. *Nanomaterials* **2020**, *10*, 1397. [CrossRef]
21. Ren, X.-Y.; Cao, J.-P.; Zhao, S.-X.; Zhao, X.-Y.; Liu, T.-L.; Feng, X.-B.; Li, Y.; Zhang, J.; Bai, H.-C. Encapsulation Ni in HZSM-5 for catalytic hydropyrolysis of biomass to light aromatics. *Fuel Process. Technol.* **2021**, *218*, 106854. [CrossRef]
22. Zhou, B.; Liu, X.; Resende, F.L.P.; Zhou, J.; Wang, M.; Dichiara, A.B. Hydropyrolysis of Residual *Camellia sinensis* and Its Cellulose and Lignin Fractions over Nickel Nanoparticles Confined Inside Carbon Nanotube Microreactors at Atmospheric Pressure. *ACS Sustain. Chem. Eng.* **2021**, *9*, 10827–10836. [CrossRef]
23. Eykelbosh, A.J.; Johnson, M.S.; Santos de Queiroz, E.; Dalmagro, H.J.; Guimarães Couto, E. Biochar from Sugarcane Filtercake Reduces Soil CO2 Emissions Relative to Raw Residue and Improves Water Retention and Nutrient Availability in a Highly-Weathered Tropical Soil. *PLoS ONE* **2014**, *9*, e98523. [CrossRef] [PubMed]
24. Vecino Mantilla, S.; Gauthier-Maradei, P.; Álvarez Gil, P.; Tarazona Cárdenas, S. Comparative study of bio-oil production from sugarcane bagasse and palm empty fruit bunch: Yield optimization and bio-oil characterization. *J. Anal. Appl. Pyrolysis* **2014**, *108*, 284–294. [CrossRef]
25. Resende, F.L.P. Recent advances on fast hydropyrolysis of biomass. *Catal. Today* **2016**, *269*, 148–155. [CrossRef]
26. Jan, O.; Marchand, R.; Anjos, L.C.A.; Seufitelli, G.V.S.; Nikolla, E.; Resende, F.L.P. Hydropyrolysis of Lignin Using Pd/HZSM-5. *Energy Fuels* **2015**, *29*, 1793–1800. [CrossRef]
27. Yu, Z.; Jiang, L.; Wang, Y.; Li, Y.; Ke, L.; Yang, Q.; Peng, Y.; Xu, J.; Dai, L.; Wu, Q.; et al. Catalytic pyrolysis of woody oil over SiC foam-MCM41 catalyst for aromatic-rich bio-oil production in a dual microwave system. *J. Clean. Prod.* **2020**, *255*, 120179. [CrossRef]
28. Zhou, Y.; Chen, Z.; Gong, H.; Wang, X.; Yu, H. A strategy of using recycled char as a co-catalyst in cyclic in-situ catalytic cattle manure pyrolysis for increasing gas production. *Waste Manag.* **2020**, *107*, 74–81. [CrossRef]
29. Yung, M.M.; Starace, A.K.; Mukarakate, C.; Crow, A.M.; Leshnov, M.A.; Magrini, K.A. Biomass Catalytic Pyrolysis on Ni/ZSM-5: Effects of Nickel Pretreatment and Loading. *Energy & Fuels* **2016**, *30*, 5259–5268. [CrossRef]
30. Persson, H.; Duman, I.; Wang, S.; Pettersson, L.J.; Yang, W. Catalytic pyrolysis over transition metal-modified zeolites: A comparative study between catalyst activity and deactivation. *J. Anal. Appl. Pyrolysis* **2019**, *138*, 54–61. [CrossRef]
31. Lu, Q.; Li, W.; Zhang, X.; Liu, Z.; Cao, Q.; Xie, X.; Yuan, S. Experimental study on catalytic pyrolysis of biomass over a Ni/Ca-promoted Fe catalyst. *Fuel* **2020**, *263*, 116690. [CrossRef]
32. Kamali, M.; Sweygers, N.; Al-Salem, S.; Appels, L.; Aminabhavi, T.M.; Dewil, R. Biochar for soil applications-sustainability aspects, challenges and future prospects. *Chem. Eng. J.* **2022**, *428*, 131189. [CrossRef]
33. Tafti, N.; Wang, J.; Gaston, L.; Park, J.; Wang, M.; Pensky, S. Agronomic and environmental performance of biochar amendment in alluvial soils under subtropical sugarcane production. *Agrosystems, Geosci. Environ.* **2021**, *4*, e20209. [CrossRef]
34. Kumar, R.; Strezov, V.; Lovell, E.; Kan, T.; Weldekidan, H.; He, J.; Dastjerdi, B.; Scott, J. Bio-oil upgrading with catalytic pyrolysis of biomass using Copper/zeolite-Nickel/zeolite and Copper-Nickel/zeolite catalysts. *Bioresour. Technol.* **2019**, *279*, 404–409. [CrossRef] [PubMed]
35. Lu, K.; Jin, F.; Wu, G.; Ding, Y. The synergetic effect of acid and nickel sites on bifunctional MWW zeolite catalysts for ethylene oligomerization and aromatization. *Sustain. Energy Fuels* **2019**, *3*, 3569–3581. [CrossRef]
36. Ma, Y.; Bao, H.; Hu, X.; Wang, R.; Dong, W. Productions of phenolic rich bio-oil using waste chilli stem biomass by catalytic pyrolysis: Evaluation of reaction parameters on products distributions. *J. Energy Inst.* **2021**, *97*, 233–239. [CrossRef]
37. Martin, N.M.; Velin, P.; Skoglundh, M.; Bauer, M.; Carlsson, P.-A. Catalytic hydrogenation of CO_2 to methane over supported Pd, Rh and Ni catalysts. *Catal. Sci. Technol.* **2017**, *7*, 1086–1094. [CrossRef]

38. Pieta, I.S.; Lewalska-Graczyk, A.; Kowalik, P.; Antoniak-Jurak, K.; Krysa, M.; Sroka-Bartnicka, A.; Gajek, A.; Lisowski, W.; Mrdenovic, D.; Pieta, P.; et al. CO_2 Hydrogenation to Methane over Ni-Catalysts: The Effect of Support and Vanadia Promoting. *Catalysts* **2021**, *11*, 433. [CrossRef]
39. Li, T.; Li, Y.; Cheng, Y.; Li, X.; Shen, Y.; Yan, L.; Wang, M.; Chang, L.; Bao, W. Effect of hydrogen-rich gas from char gasification on rapid pyrolysis products of low rank coal in a downer pyrolyzer. *RSC Adv.* **2021**, *11*, 38537–38546. [CrossRef]
40. Gupta, S.; Lanjewar, R.; Mondal, P. Enhancement of hydrocarbons and phenols in catalytic pyrolysis bio-oil by employing aluminum hydroxide nanoparticle based spent adsorbent derived catalysts. *Chemosphere* **2022**, *287*, 132220. [CrossRef]
41. Lu, Q.; Ye, X.; Zhang, Z.; Wang, Z.; Cui, M.; Yang, Y. Catalytic fast pyrolysis of sugarcane bagasse using activated carbon catalyst in a hydrogen atmosphere to selectively produce 4-ethyl phenol. *J. Anal. Appl. Pyrolysis* **2018**, *136*, 125–131. [CrossRef]
42. Stankovikj, F.; McDonald, A.G.; Helms, G.L.; Garcia-Perez, M. Quantification of Bio-Oil Functional Groups and Evidences of the Presence of Pyrolytic Humins. *Energy Fuels* **2016**, *30*, 6505–6524. [CrossRef]
43. Zhang, Y.; Lei, H.; Yang, Z.; Duan, D.; Villota, E.; Ruan, R. From glucose-based carbohydrates to phenol-rich bio-oils integrated with syngas production via catalytic pyrolysis over an activated carbon catalyst. *Green Chem.* **2018**, *20*, 3346–3358. [CrossRef]
44. Li, W.; Wang, D.; Zhu, Y.; Chen, J.; Lu, Y.; Li, S.; Zheng, Y.; Zheng, Z. Efficient ex-situ catalytic upgrading of biomass pyrolysis vapors to produce methylfurans and phenol over bio-based activated carbon. *Biomass Bioenergy* **2020**, *142*, 105794. [CrossRef]
45. Carriel Schmitt, C.; Zimina, A.; Fam, Y.; Raffelt, K.; Grunwaldt, J.-D.; Dahmen, N. Evaluation of High-Loaded Ni-Based Catalysts for Upgrading Fast Pyrolysis Bio-Oil. *Catalysts* **2019**, *9*, 784. [CrossRef]
46. He, T.; Liu, X.; Ge, Y.; Han, D.; Li, J.; Wang, Z.; Wu, J. Gas phase hydrodeoxygenation of anisole and guaiacol to aromatics with a high selectivity over Ni-Mo/SiO_2. *Catal. Commun.* **2017**, *102*, 127–130. [CrossRef]
47. Ambursa, M.M.; Juan, J.C.; Yahaya, Y.; Taufiq-Yap, Y.H.; Lin, Y.-C.; Lee, H.V. A review on catalytic hydrodeoxygenation of lignin to transportation fuels by using nickel-based catalysts. *Renew. Sustain. Energy Rev.* **2021**, *138*, 110667. [CrossRef]
48. Ramos, M.L.N.S.; Carregosa, I.S.C.; Carvalho, M.P.; da Costa, M.T.; Gagliardi, P.R.; Wisniewski, A. Potential of cattle manure pyrolysis liquid as an alternative environmentally friendly source of agricultural fungicides. *J. Anal. Appl. Pyrolysis* **2020**, *149*, 104862. [CrossRef]
49. Hertzog, J.; Carré, V.; Jia, L.; Mackay, C.L.; Pinard, L.; Dufour, A.; Mašek, O.; Aubriet, F. Catalytic Fast Pyrolysis of Biomass over Microporous and Hierarchical Zeolites: Characterization of Heavy Products. *ACS Sustain. Chem. Eng.* **2018**, *6*, 4717–4728. [CrossRef]
50. Santos, T.M.; da Silva, W.R.; Carregosa, J.d.C.; Wisniewski, A. Comprehensive characterization of cattle manure bio-oil for scale-up assessment comparing non-equivalent reactor designs. *J. Anal. Appl. Pyrolysis* **2022**, *162*, 105465. [CrossRef]
51. Michailof, C.M.; Kalogiannis, K.G.; Sfetsas, T.; Patiaka, D.T.; Lappas, A.A. Advanced analytical techniques for bio-oil characterization. *Wiley Interdiscip. Rev. Energy Environ.* **2016**, *5*, 614–639. [CrossRef]
52. Zhong, D.; Zeng, K.; Li, J.; Qiu, Y.; Flamant, G.; Nzihou, A.; Vladimirovich, V.S.; Yang, H.; Chen, H. Characteristics and evolution of heavy components in bio-oil from the pyrolysis of cellulose, hemicellulose and lignin. *Renew. Sustain. Energy Rev.* **2022**, *157*, 111989. [CrossRef]
53. Hertzog, J.; Carré, V.; Le Brech, Y.; Dufour, A.; Aubriet, F. Toward Controlled Ionization Conditions for ESI-FT-ICR-MS Analysis of Bio-Oils from Lignocellulosic Material. *Energy Fuels* **2016**, *30*, 5729–5739. [CrossRef]
54. Hita, I.; Cordero-Lanzac, T.; Kekäläinen, T.; Okafor, O.; Rodríguez-Mirasol, J.; Cordero, T.; Bilbao, J.; Jänis, J.; Castano, P. In-Depth Analysis of Raw Bio-Oil and Its Hydrodeoxygenated Products for a Comprehensive Catalyst Performance Evaluation. *ACS Sustain. Chem. Eng.* **2020**, *8*, 18433–18445. [CrossRef]
55. Palacio Lozano, D.C.; Jones, H.E.; Ramirez Reina, T.; Volpe, R.; Barrow, M.P. Unlocking the potential of biofuels via reaction pathways in van Krevelen diagrams. *Green Chem.* **2021**, *23*, 8949–8963. [CrossRef]
56. Benés, M.; Bilbao, R.; Santos, J.M.; Alves Melo, J.; Wisniewski, A.; Fonts, I. Hydrodeoxygenation of Lignocellulosic Fast Pyrolysis Bio-Oil: Characterization of the Products and Effect of the Catalyst Loading Ratio. *Energy Fuels* **2019**, *33*, 4272–4286. [CrossRef]
57. Reymond, C.; Dubuis, A.; Le Masle, A.; Colas, C.; Chahen, L.; Destandau, E.; Charon, N. Characterization of liquid–liquid extraction fractions from lignocellulosic biomass by high performance liquid chromatography hyphenated to tandem high-resolution mass spectrometry. *J. Chromatogr. A* **2020**, *1610*, 460569. [CrossRef]
58. Staš, M.; Auersvald, M.; Kejla, L.; Vrtiška, D.; Kroufek, J.; Kubička, D. Quantitative analysis of pyrolysis bio-oils: A review. *TrAC Trends Anal. Chem.* **2020**, *126*, 115857. [CrossRef]
59. Santos, L.; Silva, F.; Santos, L.; Carregosa, I.; Wisniewski Jr., A. Potential Bio-Oil Production from Invasive Aquatic Plants by Microscale Pyrolysis Studies. *J. Braz. Chem. Soc.* **2017**, *29*, 151–158. [CrossRef]
60. Ohno, T.; Ohno, P.E. Influence of heteroatom pre-selection on the molecular formula assignment of soil organic matter components determined by ultrahigh resolution mass spectrometry. *Anal. Bioanal. Chem.* **2013**, *405*, 3299–3306. [CrossRef]